nature photonics

Review article

https://doi.org/10.1038/s41566-024-01571-3

Super-resolution optical fluctuation imaging

Received: 16 June 2024

Accepted: 18 October 2024

Published online: 10 January 2025

Check for updates

Samrat Basak[1], Alexey Chizhik[1], José Ignacio Gallea[1], Ivan Gligonov[1], Ingo Gregor[1], Oleksii Nevskyi[1], Niels Radmacher[1], Roman Tsukanov[1] & Jörg Enderlein[1,2]

We present a comprehensive review of super-resolution optical fluctuation imaging (SOFI), a robust technique that leverages temporal fluctuations in fluorescence intensity to achieve super-resolution imaging without the need for single-molecule localization. The Review starts with a historical overview of super-resolution microscopy techniques, and then focuses on SOFI's core principle—the analysis of intensity fluctuations using cumulants to improve spatial resolution. The paper discusses technical challenges, such as photobleaching, blinking kinetics and pixel size limitations, as well as proposing solutions like Fourier upsampling and balanced SOFI to mitigate these issues. Additionally, we discuss potential advancements in the field, including the integration of SOFI with other super-resolution modalities like structured illumination microscopy and image scanning microscopy, and the application of SOFI in cryo-fluorescence microscopy and quantum emitter-based imaging. This paper aims to serve as an essential resource for researchers interested in utilizing SOFI for high-resolution imaging in diverse biological applications.

Fluorescence super-resolution microscopy has revolutionized the fields of cellular and molecular biology by overcoming the diffraction limit of light, which restricts the resolution of conventional optical microscopy to approximately 200 nm in the lateral plane and 500 nm in the axial plane. The first of the fluorescence super-resolution microscopy techniques to be developed is stimulated emission depletion microscopy, introduced by Stefan Hell and Jan Wichmann in 1994 (ref. 1). It uses a second laser to selectively deactivate fluorophores in the periphery of the first laser excitation spot, thereby reducing the effective point spread function (PSF) and enhancing resolution beyond the diffraction limit. This method has achieved resolutions of 20–50 nm, allowing a detailed visualization of subcellular structures.

A second class of fluorescence super-resolution methods is subsumed under the name of single-molecule localization microscopy (SMLM). SMLM uses the fact that the image of a single, isolated fluorescent molecule can be localized with a much higher precision than the width of its image (size of the PSF). SMLM is technically simpler to realize than stimulated emission depletion microscopy, and has found tremendously wide applications in the life sciences. The first two SMLM methods that were independently and quasi-simultaneously invented are photoactivated localization microscopy (PALM) and stochastic optical reconstruction microscopy (STORM). PALM, developed by Eric Betzig and Harald Hess in 2006, relies on the photoactivation and subsequent localization of individual fluorescent molecules to build a high-resolution image[2]. By sequentially activating and imaging sparse subsets of fluorophores, PALM achieves resolutions of 10–20 nm. At the same time, Xiaowei Zhuang and colleagues introduced STORM, which uses the stochastic switching of fluorescent dyes to capture the high-precision localization of individual molecules[3]. Like PALM, STORM reconstructs super-resolution images by accumulating the positions of many single-molecule events. Later, STORM was further developed into its variant called direct STORM that does not require photoswitchable proteins or dyes but uses conventional fluorophores in a reducing and oxidizing environment to induce blinking[4]. This simplifies sample preparation and maintains the high resolution.

As an important alternative to PALM, STORM and direct STORM, which rely on either irreversible or reversible photoswitching of fluorescent molecules, points accumulation for imaging in nanoscale topography (PAINT) enhances the spatial resolution by using the transient binding of fluorescent probes to their targets[5]. This method was

[1]Third Institute of Physics—Biophysics, Georg August University, Göttingen, Germany. [2]Cluster of Excellence 'Multiscale Bioimaging: from Molecular Machines to Networks of Excitable Cells' (MBExC), Universitätsmedizin Göttingen, Göttingen, Germany. e-mail: jenderl@gwdg.de

https://doi.org/10.1038/s41566-024-01571-3

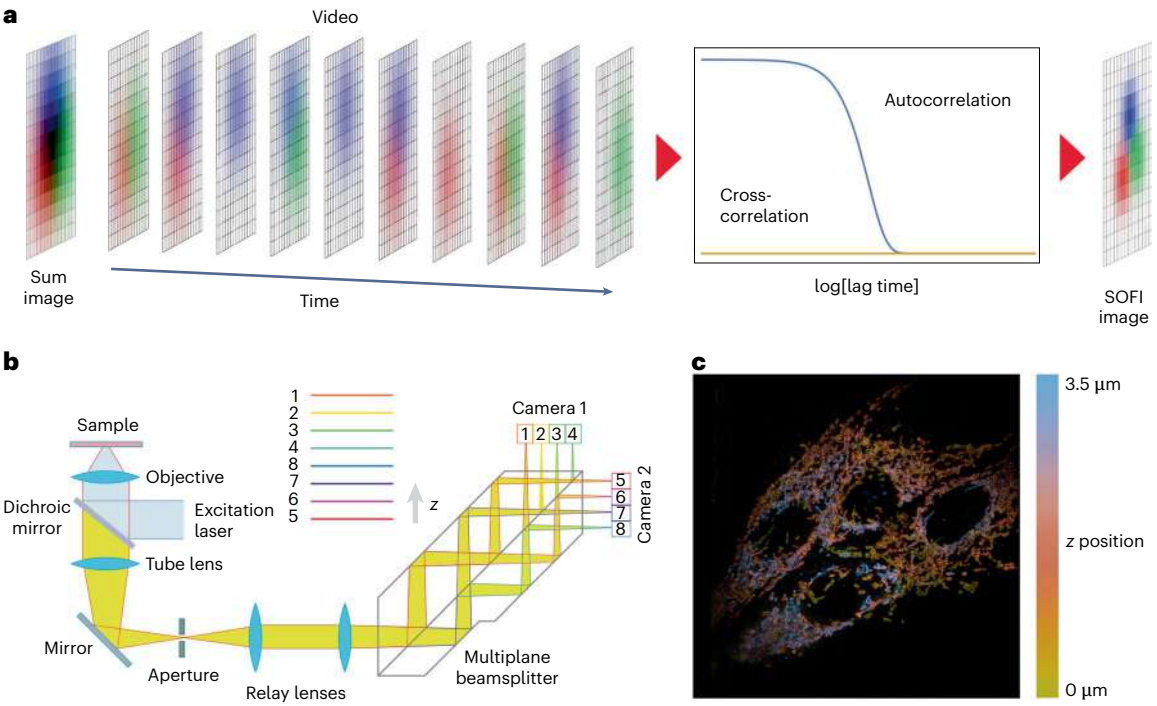

Fig. 1 | Principle of SOFI. a, Raw SOFI data are a stack of microscopy frames (video) of a sample, where the density of labels that are simultaneously in their fluorescence-on state can be much larger than what is usually acceptable in SMLM. The image shows an example of three emitters (red, green and blue) with overlapping PSFs. The sum image of the video is shown on the left, and the SOFI image obtained after pixel-wise temporal correlation is shown on the right. The frame shows a schematic of the auto- and cross-correlation of the fluorescence signal of one and between different emitters. The core ingredient of SOFI is that the cross-correlation between signals from different emitters is zero. **b**, One peculiar property of SOFI is that it imbues a wide-field microscope with confocal sectioning capability. This can be used to obtain quasi-simultaneous three-dimensional images of a sample when using a suitable multiplane imaging system as the prism-type multiplane microscope shown here. **c**, Three-dimensional SOFI imaging of mitochondria stained with Alexa 647 in fixed C2C12 cells. The maximum intensity projection of the third-order balanced SOFI image covers a volume of 65 × 65 × 3.5 µm^3 (ref. 34).

developed by the late Robin M. Hochstrasser and his coworker Alexey Sharonov, and it allows for continuous imaging unrestricted by the eventual photobleaching of the fluorescent labels. Its most widely used variant is DNA-PAINT, which uses the transient binding of short, single-stranded DNA probes (imagers) to their complementary target sequences (docking strands) attached to the structure of interest. DNA-PAINT was introduced by Ralf Jungmann and colleagues in 2010 (ref. 6), and it provides the highest spatial resolution and is particularly useful for multiplexed imaging.

The latest addition to the class of SMLM methods is minimal (fluorescence) photon flux (MINFLUX) microscopy, which was introduced by Stefan Hell and colleagues in 2016 (ref. 7). MINFLUX combines the elements of both localization and coordinate-targeted microscopy to achieve nanometre-scale resolution with fewer emitted photons compared with traditional methods[8,9].

All these SMLM methods provide the maximum optical resolution, but require the acquisition of thousands of images and the localization of millions of molecules for obtaining a decent, super-resolved image of a sample. An alternative super-resolution microscopy approach to SMLM, which also exploits the photoswitching (blinking) of fluorescent dyes but without localizing them, is super-resolution (or stochastic) optical fluctuation imaging (SOFI)[10].

SOFI has emerged as a versatile and powerful technique for overcoming the diffraction limit in fluorescence microscopy. By leveraging the temporal fluctuations of fluorescence intensity, SOFI can generate super-resolved images without the need for the precise localization of individual emitters, making it a robust alternative to STORM. This inherent flexibility allows SOFI to operate effectively even at high fluorescent label densities, which are prohibitive for SMLM, as well as to produce super-resolved images at a significantly faster rate. These attributes are particularly beneficial for live-cell imaging applications.

The advantages of SOFI are that it is extremely simple to implement, works with any label that shows any kind of intensity fluctuations and allows for the generation of super-resolved images one to two orders of magnitude faster than SMLM. Although the original publication[10] that introduced SOFI used fluorescent quantum dots for labelling, due to their intrinsic strong intensity fluctuations and high overall photostability, subsequent publications have shown that SOFI works with dyes[11], photoswitchable proteins[12,13], graphene dots[14] or exchangeable fluorophores[15].

Moreover, SOFI can be combined with other super-resolution modalities such as structured illumination microscopy (SIM)[16,17] or image scanning microscopy (ISM)[18,19], and is a promising candidate for cryo-fluorescence super-resolution microscopy. This Review provides a comprehensive overview of the working principles, performance and limitations of SOFI, as well as recent developments and advances in the technique.

Physical principle

The core idea of SOFI comes from fluorescence fluctuation spectroscopy and can be explained as follows: assume one observes stochastically blinking emitters with time-dependent intensities $s_j(t)$. If the blinking of these emitters is statistically independent from each other, then any second-order cross-cumulant $c_2[s_j(t), s_k(t+\tau)] = \langle s_j(t)s_k(t+\tau)\rangle_t - \langle s_j(t)\rangle_t\langle s_k(t)\rangle_t$ will vanish for all time differences τ (here angular brackets with subscript t denote averaging over time t). Only if both signals come from the same molecule ($j = k$), the second-order cumulant will be non-zero and equal to the temporal autocorrelation of intensity, $c_2[s_j(t), s_j(t+\tau)] = \langle s_j(t)s_j(t+\tau)\rangle_t - \langle s_j(t)\rangle^2_t$.

Now, the image recorded from a sample with n fluorescent emitters is formed by the convolution of the emitter positions with the PSF of the microscope multiplied by the corresponding intensities of the emitters:

$$I(\boldsymbol{\rho},t)=\sum_{j=1}^{n}U(\boldsymbol{\rho}-\boldsymbol{\rho}_j,z_j)s_j(t), \tag{1}$$

where $\boldsymbol{\rho}_j$ and z_j are the lateral and axial positions of the jth molecule, respectively; $s_j(t)$ is its intensity at time t; and $U(\boldsymbol{\rho}-\boldsymbol{\rho}',z')$ is the PSF, that is, the intensity generated by a molecule at lateral position $\boldsymbol{\rho}'$ and axial position z' at position $\boldsymbol{\rho}$ on the detector. For a perfectly aplanatic system, this function is indeed only a function of the difference $\boldsymbol{\rho}-\boldsymbol{\rho}'$. Now, when calculating a pixel-wise second-order cumulant along time t as

$$\begin{aligned}C_2(\boldsymbol{\rho},\tau)&=\sum_{j,k=1}^{n}U(\boldsymbol{\rho}-\boldsymbol{\rho}_j,z_j)U(\boldsymbol{\rho}-\boldsymbol{\rho}_k,z_k)C[s_j(t),s_k(t+\tau)]\\&=\sum_{j=1}^{n}U^2(\boldsymbol{\rho}-\boldsymbol{\rho}_j,z_j)c_2(\tau),\end{aligned} \tag{2}$$

the resulting second-order cumulant image $C_2(\boldsymbol{\rho},\tau)$ is only a function of detector position $\boldsymbol{\rho}$, lag time τ and the second-order temporal cumulant function $c_2(\tau)$ of the emitters' fluorescence (which is assumed to be the same for all the emitters). In particular, this image is formed by the square of the PSF. This corresponds to extending the frequency support of the optical transfer function (OTF; the Fourier transform of the PSF) by two times. A doubled frequency support of the OTF signifies a doubling of the spatial resolution, and this is the core idea of SOFI: improving the spatial resolution of the final image by performing a temporal correlation analysis of a recorded video of the raw microscopy images. It is straightforward to extend this concept beyond the second-order cumulant and to calculate an mth-order cumulant. Again, one uses the fact that the mth-order cumulant function of the stochastically fluctuating intensities of different and statistically independent emitters vanish, except if all the m intensity inputs to the mth-order cumulant come from the same molecule. Thus, the mth-order cumulant image is

$$C_m(\rho,\tau_1,\ldots,\tau_{m-1})=\sum_{j=1}^{n}U^m(\rho-\rho_j,z_j)c_m(\tau_1,\tau_2,\ldots,\tau_{m-1}), \tag{3}$$

where $c_m(\tau)$ is the mth-order temporal cumulant function of the emitters' fluorescence signal and is formed with the mth power of the PSF, signifying an m-fold improvement in spatial resolution. Here the cumulants on the left side are defined via the cumulant-generating function as

$$C_m(\boldsymbol{\rho},\tau_1,\ldots,\tau_{m-1})=\frac{\partial^m}{\partial\zeta_1\partial\zeta_2\ldots\partial\zeta_m}\ln\left\langle\exp\left[\sum_{j=1}^{m}\zeta_j I(\boldsymbol{\rho},t+\tau_{j-1})\right]\right\rangle\Bigg|_{\{\zeta_k\}=0}, \tag{4}$$

where, by definition, $\tau_0=0$. The second-, third- and fourth-order cumulant image are explicitly calculated as

$$\begin{aligned}C_2(\boldsymbol{\rho},\tau_1)&=\left\langle\prod_{j=0}^{1}[I(\boldsymbol{\rho},t+\tau_1)-\bar{I}]\right\rangle_t,\\C_3(\boldsymbol{\rho},\tau_1,\tau_2)&=\left\langle\prod_{j=0}^{2}[I(\boldsymbol{\rho},t+\tau_1)-\bar{I}]\right\rangle_t,\\C_4(\boldsymbol{\rho},\tau_1,\tau_2,\tau_3)&=\left\langle\prod_{j=0}^{2}[I(\boldsymbol{\rho},t+\tau_1)-\bar{I}]\right\rangle_t-C_2(\boldsymbol{\rho},\tau_1)C_2(\boldsymbol{\rho},\tau_3-\tau_2)-\\&\quad-C_2(\boldsymbol{\rho},\tau_2)C_2(\boldsymbol{\rho},\tau_3-\tau_1)-C_2(\boldsymbol{\rho},\tau_3)C_2(\boldsymbol{\rho},\tau_2-\tau_1),\end{aligned} \tag{5}$$

where the average intensity image $\bar{I}$ is defined as

$$\bar{I}=\langle I(\boldsymbol{\rho},t)\rangle_t. \tag{6}$$

Finally, one can integrate over all the possible times $0<\tau_j<\infty$ for obtaining a final super-resolved cumulant image. This idea was first presented and verified in a study in 2009, where it was demonstrated by analysing the temporal intensity fluctuations of fluorescent quantum dots and SOFI was demonstrated up to the 25th order[10]. Meanwhile, different open-source software tools for performing, testing and modelling SOFI are freely available[20–22].

Optical resolution and pixel size

As explained in the previous section, an mth-order SOFI image is formed with the mth power of the PSF $U(\mathbf{r})$ (Fig. 2, second column). In Fourier space, this corresponds to an m-fold autoconvolution of the OTF $\tilde{U}(\mathbf{k})$, or

$$\tilde{U}^{(m)}_{\mathrm{SOFI}}(\mathbf{k})=\underbrace{\tilde{U}(\mathbf{k})\otimes\tilde{U}(\mathbf{k})\otimes\ldots\otimes\tilde{U}(\mathbf{k})}_{m\text{ times}}, \tag{7}$$

which results in an m-fold extension of the frequency support of the OTF of the used microscope (Fig. 2, left column). However, the apparent resolution improvement will be only a factor of $\sqrt{m}$, which corresponds to a decrease in width of the mth power of the PSF. As detailed in another work[23], this does not produce the optimal PSF for the 'sharpest' image. In that work, the optimal PSF was defined as being positive everywhere, with a maximum peak value, or equivalently, a maximum integral value of the OTF over its support. This paper demonstrates that for a given finite frequency support of an OTF (set of all non-zero spatial frequencies), the optimal OTF is the autoconvolution of a uniform amplitude distribution.

To illustrate this for the second-order SOFI, the PSF (Fig. 2, second panel in the second row) is the square of the wide-field microscope's PSF (Fig. 2, second panel in the first row). Accordingly, the OTF for the second-order SOFI (Fig. 2, first panel in the second row) is the autoconvolution of wide-field microscope's OTF (Fig. 2, first panel in the first row). On the basis of the aforementioned principles of an ideal OTF, the optimal OTF for the second-order SOFI (Fig. 2, third panel in the second row) is given by the autoconvolution of a uniform frequency distribution over the wide-field OTF's frequency support (Fig. 2, third panel in the first row). In particular, this is also the ideal OTF of a confocal microscope with a zero-diameter pinhole, which is equivalent to the ideal OTF of $\tilde{U}_{\mathrm{ISM}}$ (refs. 24,25).

For the mth-order SOFI, its OTF is the mth autoconvolution of the wide-field OTF, resulting in an mth-fold extended frequency support in all directions compared with the wide-field OTF. Analogous to the case of the second-order SOFI with doubled frequency support, the optimal OTF for the mth-order SOFI is given (for $m>1$) by

$$\tilde{U}^{(m)}_{\mathrm{SOFI,\,ideal}}(\mathbf{k})=\tilde{U}_{\mathrm{ISM}}\left(\frac{2\mathbf{k}}{m}\right), \tag{8}$$

which is shown in the third column in Fig. 2. To achieve this in SOFI, one has to reweigh the Fourier amplitudes of a SOFI image $\tilde{I}^{(m)}_{\mathrm{SOFI}}(\mathbf{k})$ by

$$\tilde{I}^{(m)}_{\mathrm{SOFI,\,ideal}}(\mathbf{k})=\frac{\tilde{U}_{\mathrm{ISM}}(2\mathbf{k}/m)}{\varepsilon+\tilde{U}(\mathbf{k})\otimes\tilde{U}(\mathbf{k})\otimes\ldots\otimes\tilde{U}(\mathbf{k})}\tilde{I}^{(m)}_{\mathrm{SOFI}}(\mathbf{k}), \tag{9}$$

where ε is a sufficiently small constant that prevents unwanted noise amplification at high spatial frequencies for which the m-fold autoconvolution in the denominator approaches zero. Typically, one chooses ε to be ~0.1 of the maximum absolute value of this autoconvolution, which still allows to nearly achieve the full potentially possible resolution (Fig. 2, fourth column) without introducing significant noise artefacts. Certainly, more sophisticated frequency readjustment algorithms are

https://doi.org/10.1038/s41566-024-01571-3

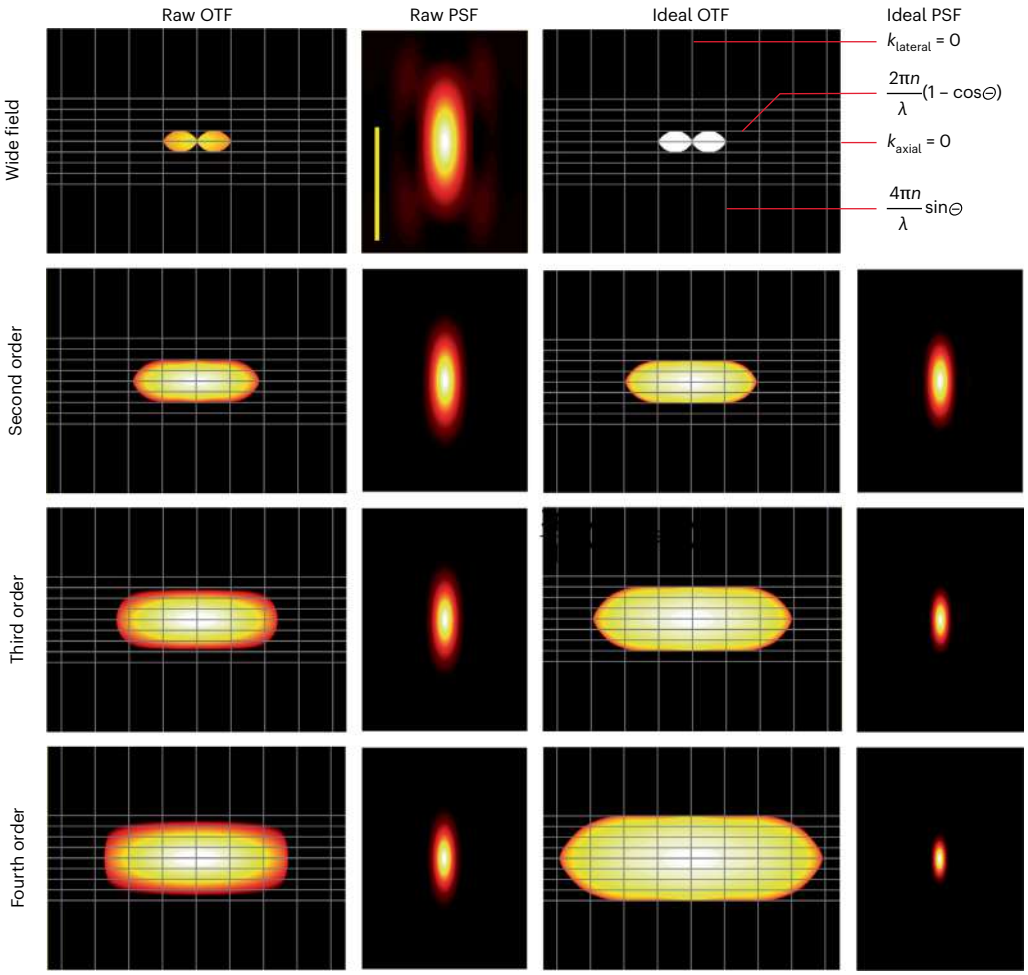

Fig. 2 | OTF and PSF of SOFI. The left column shows the lateral–axial cross-sections (logarithmic density plots) of the OTFs for a wide-field microscope (top) and for the second- to fourth-order SOFI, as obtained when applying the corresponding correlation analysis to the signals recorded by the camera pixels. The second column shows the lateral–axial cross-sections (linear density plots) of the resulting PSFs, where the vertical yellow bar in the top panel corresponds to 1 µm. The second panel of the third column shows the ideal OTF for the second-order SOFI, which is obtained by autoconvolving the OFT of a wide-field microscope but with all the non-zero amplitudes set to zero, as shown in the first panel of the third column. The ideal OTFs for the third- and fourth-order SOFI, as shown in the third and fourth panels of the third column, are rescaled versions of the ideal OTF of the second-order SOFI. The fourth column shows the resulting PSFs for the different SOFI orders. The vertical and horizontal grey lines show the maximum extent of the frequency support of the different OTFs (also shown as the annotation on the top right), where λ is the emission wavelength, n is the sample's (microscope's immersion medium) refractive index and Θ is the maximum half-angle of light collection of the used microscope objective. The PSFs were calculated for an emission wavelength λ of 500 nm.

possible, which could also take into account the actual noise level in an image[26,27], and this is one of the ongoing research efforts in SOFI. Of course, as seen by comparing the 'raw' and ideal OTFs for different SOFI orders (Fig. 2, first and third columns), the higher the SOFI order, the faster the Fourier amplitudes decay at higher spatial frequencies, which increasingly reduces the ability to reach the full m-fold resolution enhancement that is theoretically possible with the mth-order SOFI.

One of the technical issues in the early years of SOFI was the discrepancy between the achievable resolution by higher-order SOFI and the finite pixel size of the camera used to capture the raw images. In other words, the theoretically achievable resolution of SOFI could easily surpass the effective pixel size of the recorded images. One solution to this problem is to use cross-correlation between adjacent pixels to generate intermediate pixels in the final SOFI image. Temporal cross-correlation of signals from different pixels has the advantage of utilizing the zero-lag-time contribution of the temporal correlation, which leads to shot-noise artefacts in a one-pixel autocorrelation analysis. However, generating intermediate pixels by pixel cross-correlation may lead to pixelation artefacts, which can be corrected using dedicated correction algorithms[28].

An alternative and artefact-free solution to the pixel size problem is Fourier-upsampling SOFI[29], a lossless and exact interpolation method for data with finite spatial-frequency support. In Fourier upsampling, a two-dimensional Fourier transform of the recorded raw images is first performed. If the original image size is large enough and the pixel size is small enough to fully sample the PSF according to the Nyquist criterion (typically corresponding to an effective pixel size of approximately 50–100 nm), the Fourier-transformed image will clearly show the limited frequency support of the OTF, beyond which the Fourier amplitudes are close to zero (noise).

By padding the Fourier image with a sufficiently wide margin of zeros and then transforming the image back to real space, images with arbitrarily small pixel sizes can be generated without distorting the image content. These images can then be used for SOFI analysis, allowing for super-resolved images with a pixel size matching the maximum resolution of the given SOFI order.

Core imaging properties

SOFI has several attractive properties. First, it does not require the identification and localization of individual emitters, though it still needs

stochastic photoswitching or blinking, allowing it to work at fluorescent label densities that would be prohibitive for SMLM. As a result, SOFI can generate super-resolved images faster than conventional SMLM, which is particularly beneficial for live-cell imaging. A comprehensive comparison between SOFI and SMLM[30] highlights the advantages and limitations of both methods in terms of resolution, imaging speed and label density. In this vein, an interesting synthesis of SOFI and SMLM was presented earlier[31], where the authors demonstrated how SOFI can improve image generation in SMLM by contributing to the elimination of the background noise and false positives in single-molecule localization.

Second, SOFI removes any background (autofluorescence and scattering) that does not fluctuate over time from an image[32]. Third, even second-order SOFI, which generates images with the square of the PSF, induces optical sectioning[33], similar to confocal or two-photon excitation scanning microscopy. This capability allows images to be taken with a conventional wide-field microscope, which lacks intrinsic optical sectioning capability. Several earlier works have cleverly combined this capability with multiplane-imaging wide-field microscopy to generate quasi-simultaneous three-dimensional images with nearly tripled resolution in all directions[34–36]. An alternative approach that leverages the sectioning capability of SOFI to generate three-dimensional images in one step was presented by Purohit et al.[37]. They used a helical wavefront shaper[38] to generate a double-helix PSF, which was then used with a spatiotemporal correlation analysis to obtain super-resolved three-dimensional images of a sample.

Fourth, SOFI does not require special on/off kinetics of fluorescence blinking (as usually needed for SMLM) and, thus, works with any emitter that exhibits stochastic blinking. The first realizations of SOFI were performed with fluorescent quantum dots due to their stochastic and spontaneous blinking over a wide range of timescales. Later, SOFI was demonstrated with organic fluorescent dyes[36], photoswitchable fluorescent proteins[39], blinking carbon nanodots[14] and blinking polymer nanoparticles[40,41]. Similar to PAINT imaging, the intensity fluctuations induced by the reversible binding of fluorophores to target sites can also be used for SOFI[15,42].

Cusp artefacts, photobleaching, statistics and nonlinearities

A peculiarity of SOFI is that the final image quality depends not only on the fluorescence intensity and the number of recorded raw images but also on the cumulant order and blinking kinetics. For unfavourable on/off blinking kinetics parameters, certain orders of SOFI may exhibit cusp artefacts, resulting in a nearly dark image with close-to-zero contrast[43]. This issue was extensively studied in ref. 44, where the authors analysed which blinking kinetics, SOFI order and alternative fluctuation analysis approaches help avoid such artefacts. An interesting method to prevent cusp artefacts and optimize the blinking behaviour of fluorescent emitters was presented by Xu et al., who used photoswitchable fluorescent proteins and tuned their blinking behaviour with an additional light source[45]. Using this approach, they demonstrated that only 20 raw images are sufficient for obtaining decent SOFI images, enabling them to observe the dynamics of the endoplasmic reticulum in living cells.

SOFI assumes strict stationarity of a sample's fluorescence signal, meaning that the statistical properties of the signal do not change over time. However, in real samples, photobleaching of fluorescent labels is unavoidable, which can introduce artefacts into the final SOFI image[46]. One obvious way to mitigate this is to repeatedly apply the SOFI algorithm to short substacks of the full recorded video so that photobleaching over the acquisition time of one substack is negligible. Another very promising approach to avoid photobleaching artefacts is the use of exchangeable fluorophores[15], similar to what is done in PAINT[5,47] for lifting the restrictions imposed by photobleaching on SMLM. Such labels are now even available as protein tags compatible with in-cell live-cell microscopy[48]. More sophisticated approaches correct the recorded fluorescence images for photobleaching before SOFI analysis[46,49]. Interestingly, when applying a suitably modified algorithm, photobleaching can even be used as the core 'fluctuation' mechanism for SOFI, as demonstrated in ref. 50.

Additionally, the free diffusion of fluorescent dyes may affect the final SOFI result, an effect extensively studied in ref. 51. There, the authors investigated how the diffusion of fluorescent probes impacts the performance of SOFI, motivated by the increasing use of SOFI in live-cell fluorescence imaging, where dynamic processes, such as diffusion, may distort the imaging results. The authors developed a theoretical model to describe SOFI in the presence of diffusing emitters and validated this through numerical simulations. They focused on the diffusion of fluorophores in biological systems, particularly in membrane microdomains, and examined how diffusion alters the SOFI signal. The results showed that although diffusion does affect the SOFI signal, it improves spatial sampling, thereby enhancing the image quality. The extent of image distortion depended on diffusion coefficients and the on-time ratio of the fluorophores. The authors concluded that in practical biological experiments, the distortion caused by diffusion is minimal and can even be beneficial by reducing spatial undersampling, thereby improving the overall image accuracy.

To obtain sufficiently good statistics when calculating the cumulant images from the temporal averages of recorded videos, the required length of the recorded videos grows nonlinearly with increasing cumulant order. Thus, in most situations, SOFI will be restricted to a maximum of the fourth order, typically requiring several thousand recorded images to achieve a decent final image. The question arises of how to quantitatively judge the reliability and quality of the final SOFI image obtained from a finite number of recorded raw images. One answer was provided by Vandenberg et al.[52], who presented a strategy for estimating the variance (uncertainty) associated with each pixel in a SOFI image. Similarly, Wang et al.[53] and Cevoli et al.[54] conducted thorough statistical analyses of the achievable signal-to-noise ratio in SOFI image formation as a function of SOFI order, blinking kinetics, image acquisition frame rate, number of recorded frames and fluorescence intensity. For obtaining decent SOFI images, camera systems with sufficient detection efficiency and low background are important. An in-depth comparative study of different camera types (electron-multiplying charge-coupled device and scientific complementary metal–oxide–semiconductor) for their suitability for SOFI was presented in ref. 44.

An important and not fully solved issue with SOFI is that an emitter contributes with the mth power of its average intensity to an mth-order SOFI image. This leads to considerable nonlinearity in the final image: for example, in a third-order SOFI image, an emitter contributes only about 11% as much as an emitter that is twice as bright. One potential solution to this problem is balanced SOFI[20], which applies an additional global deconvolution using several orders of SOFI images to linearize the intensity of the SOFI image. However, the quality and performance of this procedure strongly depend on the label density and are difficult to calibrate. Nonetheless, balanced SOFI has the advantage of providing additional information such as molecular-state lifetimes, as well as concentration and brightness distributions of fluorophores.

Extensions and modifications

An interesting extension of SOFI is to use emitter blinking not only to increase the spatial resolution but also to evaluate blinking kinetics for distinguishing between different emitter types, thereby enabling image multiplexing. This approach was demonstrated with photoswitchable fluorescent proteins by Duwé et al.[13]. Related work includes studies by Kisley et al.[55] and Chatterjee et al.[56], who combined classical fluorescence correlation spectroscopy with SOFI to achieve higher spatial resolution as well as learning about local diffusion in complex samples.

https://doi.org/10.1038/s41566-024-01571-3

Similarly, Lukes et al.[57] used fluorescence-correlation-spectroscopy-like analysis with SOFI to estimate the number of proteins at specific positions within a SOFI image. Hertel et al.[58] used SOFI and additional fluctuation analysis to elucidate protein–protein interactions in live cells with enhanced spatial resolution.

In recent years, substantial efforts have been devoted to improving and accelerating the SOFI algorithm to enhance the imaging speed and image quality. Jiang et al. removed low-frequency fluctuations and readout noise from raw images using wavelet-based filters[59], enabling them to speed up SOFI image generation by a factor of ten. Zhou et al. used a low-pass denoising step before cumulant analysis to achieve higher image quality and speed with higher-order SOFI[60]. Zhao et al. achieved remarkable improvements in SOFI performance[61] by incorporating pre- and post-processing image deconvolution steps, reducing the number of image frames required for a final second-order SOFI image with approximately 130 nm lateral resolution by nearly two orders of magnitude.

Multiplexing is a crucial aspect of microscopy techniques, allowing for the simultaneous imaging of several different targets. One approach for multiplexing is to acquire images in different spectral channels and then apply SOFI to each recorded colour. Grußmayer et al.[62] demonstrated that dual-colour recording combined with a colour cross-correlation SOFI algorithm can simultaneously unmix more than two colours, paving the way for highly multiplexed SOFI.

A fascinating extension of SOFI is its combination with super-resolution techniques that use structured illumination and wide-field detection (SIM and ISM). Zhao et al. theoretically analysed this combination in ref. 63, and Descloux et al. experimentally realized it[64], combining SOFI with rapid SIM and SOFI with multifocus ISM, resulting in a nearly doubled image resolution. Similarly, Sroda et al. combined SOFI and ISM (SOFISM)[65] using a confocal laser scanning microscope extended with a small ultrafast array detector for image acquisition. Technically similar, Xu et al. used a commercial ISM microscope (AiryScan from Carl Zeiss Jena) to achieve an impressive second-order SOFI resolution of 91 nm (ref. 45). An alternative to improving resolution through structured illumination with a periodic stripe pattern (SIM) or with a focused laser beam (ISM) is to use random or speckle illumination. Choi et al. used such an approach with SOFI to increase the resolution of second-order SOFI to 2.8 (ref. 66).

A particularly intriguing variant of SOFI exploits fluctuations induced by quantum correlations of fluorescence emission in the nanosecond time range (fluorescence antibunching). By measuring the autocorrelation of a single emitter with subnanosecond temporal resolution, a characteristic anticorrelation (antibunching) with a correlation time determined by the fluorescence lifetime and excitation rate is observed, which can also be used to generate a SOFI image. This method was pioneered by the group of Oron[67–69], who used an optical-fibre-bundle coupled single-photon avalanche diode array for image recording. The method has become much simpler with the availability of single-photon avalanche diode array detectors[70], which promise to revolutionize this kind of imaging. Although the method is a priori slow due to the need to collect sufficient photon-pair correlations on the nanosecond timescale, sophisticated data analysis and image reconstruction have accelerated image formation by orders of magnitude[71].

An exciting prospect for SOFI is its application in cryo-fluorescence super-resolution microscopy. Cryo-fluorescence microscopy is crucial in correlative light and electron microscopy, where fluorescence imaging complements the exceptional resolution of electron microscopy. However, the resolution gap between conventional fluorescence and electron microscopy presents a challenge, and many attempts have been made to apply super-resolution techniques such as stimulated emission depletion or SMLM at liquid-nitrogen or liquid-helium temperatures. At these temperatures, most photophysical transitions are either greatly slowed down or completely frozen, which has so far impeded the achievement of super-resolution fluorescence imaging under cryogenic conditions (with very few exceptions[72–76]). SOFI could offer an interesting alternative as it does not require controlled photoswitching with long on and off times but can use any intensity fluctuations. A proof-of-principle demonstration of this idea was provided by Moser et al.[77].

A noteworthy variant of SOFI is super-resolution radial fluctuation (SRRF) microscopy, which applies a radial intensity gradient algorithm to an image before performing the SOFI fluctuation analysis[78]. A downside of this method is the lack of a clear mathematical model for the resulting PSF or OTF of SRRF (in contrast to SOFI, see ref. 79), making it difficult to assess the reliability and achievable resolution

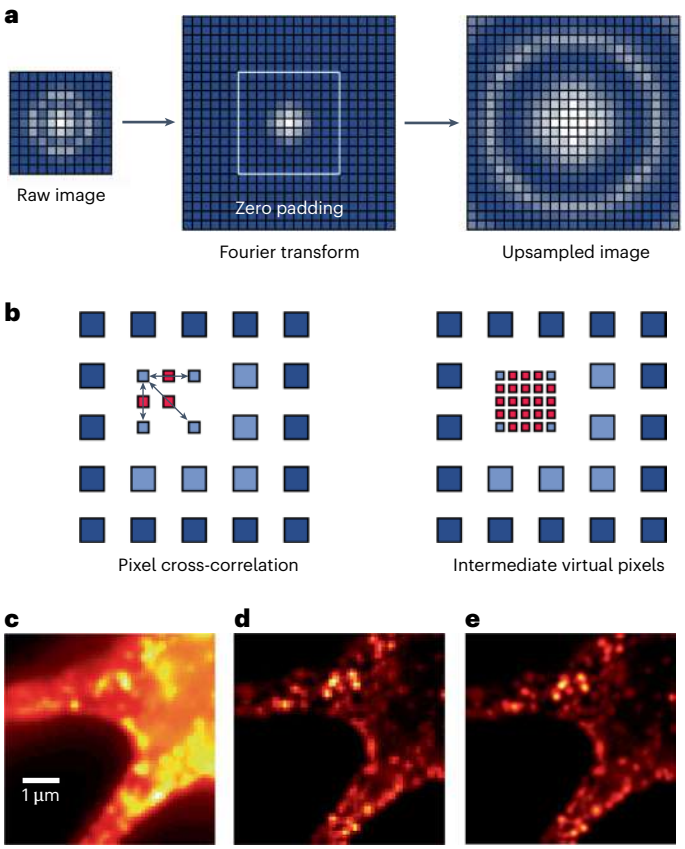

Fig. 3 | Pixel size problem. One technical issue with SOFI is that the theoretically achievable resolution can be better than the pixel size of the raw images. To solve this contradiction, two different approaches can be used. **a**, In Fourier upsampling, one first transforms the raw images into Fourier space, where they have limited spectral support due to the finite resolution of the microscope. This allows for padding the Fourier transform with zeros without altering the image content, and back-transforming this zero-padded Fourier transform to real space results in an image with increased pixel numbers and reduced pixel size. **b**, The alternative is to calculate not only the temporal correlations of the signal of the same pixel but also cross-correlations of signals between neighbouring pixels, which results in virtual intermediate SOFI pixels. **c**, Example of Fourier-upsampling SOFI. Sum image of a rat hippocampal neuron with neurotransmitter receptor subunit $GABA_BR1$ immunostained with commercial quantum dots QD525 (Invitrogen). The raw stack of images contains 3,000 frames recorded at a 20 Hz frame rate. Fluorescence was excited at a 401 nm wavelength and about 20 W cm^{-2} using a laser (Cube401, 100 mW, Coherent). The microscope used was a commercial epifluorescence microscope (IX71, Olympus) equipped with a 1.4 oil-immersion objective (UPlanSApo, Olympus) and an electron-multiplying charge-coupled device (DU-897-CS0-BV, Andor). Magnification was chosen in such a way that the effective pixel size of the recorded images was 100 nm. Fluorescent light was filtered from the excitation light using a dichroic beamsplitter (FF444/520/590, Semrock). **d**, Second-order SOFI. **e**, Second-order SOFI after 3× Fourier upsampling.

of the final images. Nonetheless, SRRF has gained popularity in the super-resolution community[80–90] because it promises faster imaging by seemingly requiring fewer raw images to obtain a final super-resolved image. It remains to be seen whether a quantitative and exact model of SRRF image formation can be developed to assess the method's reliability and accuracy.

Conclusion

We have presented a concise overview on SOFI, its different variants, applications and remaining technical issues. Despite its advantages, SOFI is not without challenges. Issues such as cusp artefacts resulting from unfavourable blinking kinetics, the impact of photobleaching and the effects of dye diffusion have been extensively studied. Solutions based on photoswitchable fluorescent proteins, Fourier upsampling and advanced fluctuation analysis have been proposed to mitigate these issues. Moreover, improvements in SOFI algorithms, such as wavelet-based filtering and pre- and post-processing deconvolution steps, have significantly enhanced the imaging speed and quality.

The ability of SOFI to multiplex by distinguishing different emitter types based on their blinking kinetics opens new avenues for complex biological imaging. Combining SOFI with other super-resolution techniques, such as SIM and ISM, has demonstrated further improvements in resolution and imaging capabilities. Additionally, innovative approaches utilizing quantum correlations and cryo-fluorescence microscopy are pushing the boundaries of what can be achieved with SOFI.

In conclusion, SOFI stands out as a highly adaptable and efficient super-resolution technique, offering significant advantages in terms of imaging speed, flexibility and multiplexing capabilities. Ongoing advancements and innovative applications continue to expand the scope and utility of SOFI, solidifying its role as a critical tool in the field of fluorescence microscopy. Future work will undoubtedly focus on further refining SOFI methodologies, improving image quality and expanding its application to new and challenging biological systems.

References

1. Hell, S. W. & Wichmann, J. Breaking the diffraction resolution limit by stimulated emission: stimulated-emission-depletion fluorescence microscopy. *Opt. Lett.* **19**, 780–782 (1994).
2. Betzig, E. et al. Imaging intracellular fluorescent proteins at nanometer resolution. *Science* **313**, 1642–1645 (2006).
3. Rust, M. J., Bates, M. & Zhuang, X. Sub-diffraction-limit imaging by stochastic optical reconstruction microscopy (STORM). *Nat. Methods* **3**, 793–795 (2006).
4. Heilemann, M. et al. Subdiffraction-resolution fluorescence imaging with conventional fluorescent probes. *Angew. Chem. Int. Ed.* **47**, 6172–6176 (2008).
5. Sharonov, A. & Hochstrasser, R. M. Wide-field subdiffraction imaging by accumulated binding of diffusing probes. *Proc. Natl Acad. Sci. USA* **103**, 18911–18916 (2006).
6. Jungmann, R. et al. Single-molecule kinetics and super-resolution microscopy by fluorescence imaging of transient binding on DNA origami. *Nano Lett.* **10**, 4756–4761 (2010).
7. Schmidt, R. et al. Minflux: low-light nanoscopy with molecular resolution. *Nat. Methods* **13**, 339–342 (2016).
8. Balzarotti, F. et al. Nanometer resolution imaging and tracking of fluorescent molecules with minimal photon fluxes. *Science* **355**, 606–612 (2017).
9. Gwosch, K. et al. MINFLUX nanoscopy delivers 3D multicolor nanometer resolution in cells. *Nat. Methods* **17**, 217–224 (2020).
10. Dertinger, T., Colyer, R., Iyer, G., Weiss, S. & Enderlein, J. Fast, background-free, 3D super-resolution optical fluctuation imaging (SOFI). *Proc. Natl Acad. Sci. USA* **106**, 22287–22292 (2009).
11. Dertinger, T., Heilemann, M., Vogel, R., Sauer, M. & Weiss, S. Super-resolution optical fluctuation imaging with organic dyes. *Angew. Chem. Int. Ed.* **49**, 9441–9443 (2010).
12. Duwé, S., Moeyaert, B. & Dedecker, P. Diffraction-unlimited fluorescence microscopy of living biological samples using pcSOFI. *Curr. Protoc. Chem. Biol.* **7**, 27–41 (2015).
13. Duwé, S., Vandenberg, W. & Dedecker, P. Live-cell monochromatic dual-label sub-diffraction microscopy by mt-pcSOFI. *Chem. Commun.* **53**, 7242–7245 (2017).
14. Chizhik, A. M. et al. Super-resolution optical fluctuation bio-imaging with dual-color carbon nanodots. *Nano Lett.* **16**, 237–242 (2016).
15. Glogger, M., Spahn, C., Enderlein, J. & Heilemann, M. Multi-color, bleaching-resistant super-resolution optical fluctuation imaging with oligonucleotide-based exchangeable fluorophores. *Angew. Chem. Int. Ed.* **133**, 6380–6383 (2021).
16. Gustafsson, M. G. Extended resolution fluorescence microscopy. *Curr. Opin. Struct. Biol.* **9**, 627–628 (1999).
17. Heintzmann, R. & Huser, T. Super-resolution structured illumination microscopy. *Chem. Rev.* **117**, 13890–13908 (2017).
18. Sheppard, C. J. Super-resolution in confocal imaging. *Optik* **80**, 53–54 (1988).
19. Müller, C. B. & Enderlein, J. Image scanning microscopy. *Phys. Rev. Lett.* **104**, 198101 (2010).
20. Geissbuehler, S. et al. Mapping molecular statistics with balanced super-resolution optical fluctuation imaging (bSOFI). *Opt. Nano.* **1**, 4 (2012).
21. Girsault, A. et al. SOFI simulation tool: a software package for simulating and testing super-resolution optical fluctuation imaging. *PLoS ONE* **11**, e0161602 (2016).
22. Miao, Y., Weiss, S. & Yi, X. PySOFI: an open source Python package for SOFI. *Biophys. Rep.* **2**, 100052 (2022).
23. Stallinga, S., Radmacher, N., Delon, A. & Enderlein, J. Optimal transfer functions for bandwidth-limited imaging. *Phys. Rev. Res.* **4**, 023003 (2022).
24. Radmacher, N. et al. Doubling the resolution of fluorescence-lifetime single-molecule localization microscopy with image scanning microscopy. *Nat. Photon.* https://doi.org/10.1038/s41566-024-01481-4 (2024).
25. Fazel, M. et al. Fluorescence microscopy: a statistics-optics perspective. *Rev. Mod. Phys.* **96**, 025003 (2024).
26. Smith, C. S. et al. Structured illumination microscopy with noise-controlled image reconstructions. *Nat. Methods* **18**, 821–828 (2021).
27. Rieger, B., Droste, I., Gerritsma, F., Brink, T. T. & Stallinga, S. Single image Fourier ring correlation. *Opt. Express* **32**, 21767–21782 (2024).
28. Bierbuesse, F., Gielen, V., Vandenberg, W. & Dedecker, P. Model-free pixelation correction in SOFI imaging. *OSA Contin.* **4**, 77–86 (2021).
29. Stein, S. C., Huss, A., Hähnel, D., Gregor, I. & Enderlein, J. Fourier interpolation stochastic optical fluctuation imaging. *Opt. Express* **23**, 16154–16163 (2015).
30. Deschout, H. et al. Complementarity of PALM and SOFI for super-resolution live-cell imaging of focal adhesions. *Nat. Commun.* **7**, 13693 (2016).
31. Schidorsky, S. et al. Synergizing superresolution optical fluctuation imaging with single molecule localization microscopy. *Methods Appl. Fluoresc.* **6**, 045008 (2018).
32. Dertinger, T., Colyer, R., Vogel, R., Enderlein, J. & Weiss, S. Achieving increased resolution and more pixels with superresolution optical fluctuation imaging (SOFI). *Opt. Express* **18**, 18875–18885 (2010).
33. Dertinger, T., Xu, J., Naini, O., Vogel, R. & Weiss, S. SOFI-based 3D superresolution sectioning with a widefield microscope. *Opt. Nano.* **1**, 2 (2012).
34. Geissbuehler, S. et al. Live-cell multiplane three-dimensional super-resolution optical fluctuation imaging. *Nat. Commun.* **5**, 5830 (2014).

35. Descloux, A. et al. Combined multi-plane phase retrieval and super-resolution optical fluctuation imaging for 4D cell microscopy. *Nat. Photon.* **12**, 165–172 (2018).
36. Grußmayer, K., Lukes, T., Lasser, T. & Radenovic, A. Self-blinking dyes unlock high-order and multiplane super-resolution optical fluctuation imaging. *ACS Nano* **14**, 9156–9165 (2020).
37. Purohit, A. et al. Spatio-temporal correlation super-resolution optical fluctuation imaging. *Eur. Phys. Lett.* **125**, 20005 (2019).
38. Pavani, S. R. P. et al. Three-dimensional, single-molecule fluorescence imaging beyond the diffraction limit by using a double-helix point spread function. *Proc. Natl Acad. Sci. USA* **106**, 2995–2999 (2009).
39. Zhang, X. et al. Development of a reversibly switchable fluorescent protein for super-resolution optical fluctuation imaging (SOFI). *ACS Nano* **9**, 2659–2667 (2015).
40. Liu, Z. et al. Narrow-band polymer dots with pronounced fluorescence fluctuations for dual-color super-resolution imaging. *Nanoscale* **12**, 7522–7526 (2020).
41. Li, W., Kaminski Schierle, G. S., Lei, B., Liu, Y. & Kaminski, C. F. Fluorescent nanoparticles for super-resolution imaging. *Chem. Rev.* **122**, 12495–12543 (2022).
42. Zeng, Z. et al. Fast super-resolution imaging with ultra-high labeling density achieved by joint tagging super-resolution optical fluctuation imaging. *Sci. Rep.* **5**, 8359 (2015).
43. Yi, X. & Weiss, S. Cusp-artifacts in high order superresolution optical fluctuation imaging. *Biomed. Opt. Express* **11**, 554 (2020).
44. Eynde, R. V. D. et al. Quantitative comparison of camera technologies for cost-effective super-resolution optical fluctuation imaging (SOFI). *J. Phys. Photon.* **1**, 044001 (2019).
45. Xue, F. et al. SOGO-SOFI, light-modulated super-resolution optical fluctuation imaging using only 20 raw frames for high-fidelity reconstruction. *Fundam. Res.* https://doi.org/10.1016/j.fmre.2023.03.007 (2023).
46. Peeters, W. et al. Correcting for photodestruction in super-resolution optical fluctuation imaging. *Sci. Rep.* **7**, 10470 (2017).
47. Jungmann, R. et al. Quantitative super-resolution imaging with qPAINT. *Nat. Methods* **13**, 439–442 (2016).
48. Kompa, J. et al. Exchangeable HaloTag ligands for super-resolution fluorescence microscopy. *J. Am. Chem. Soc.* **145**, 3075–3083 (2023).
49. Hugelier, S. et al. Smoothness correction for better SOFI imaging. *Sci. Rep.* **11**, 7569 (2021).
50. Brutkowski, W., Dziob, D. & Bernas, T. Increasing microscopy resolution with photobleaching and intensity cumulant analysis. *Microsc. Res. Tech.* **78**, 958–968 (2015).
51. Vandenberg, W., & Dedecker, P. Effect of probe diffusion on the SOFI imaging accuracy. *Sci. Rep.* **7**, 44665 (2017).
52. Vandenberg, W. et al. Model-free uncertainty estimation in stochastical optical fluctuation imaging (SOFI) leads to a doubled temporal resolution. *Biomed. Opt. Express* **7**, 467–480 (2016).
53. Wang, X., Chen, D., Yu, B. & Niu, H. Statistical precision in super-resolution optical fluctuation imaging. *Appl. Opt.* **55**, 7911–7916 (2016).
54. Cevoli, D. et al. Design of experiments for the optimization of SOFI super-resolution microscopy imaging. *Biomed. Opt. Express* **12**, 2617–2630 (2021).
55. Kisley, L. et al. Characterization of porous materials by fluorescence correlation spectroscopy super-resolution optical fluctuation imaging. *ACS Nano* **9**, 9158–9166 (2015).
56. Chatterjee, S., Kramer, S. N., Wellnitz, B., Kim, A. & Kisley, L. Spatially resolving size effects on diffusivity in nanoporous extracellular matrix-like materials with fluorescence correlation spectroscopy super-resolution optical fluctuation imaging. *J. Phys. Chem. B* **127**, 4430–4440 (2023).
57. Lukeš, T. et al. Quantifying protein densities on cell membranes using super-resolution optical fluctuation imaging. *Nat. Commun.* **8**, 1731 (2017).
58. Hertel, F., Mo, G. C. H., Duwé, S., Dedecker, P. & Zhang, J. RefSOFI for mapping nanoscale organization of protein-protein interactions in living cells. *Cell Rep.* **14**, 390–400 (2016).
59. Jiang, S. et al. Enhanced SOFI algorithm achieved with modified optical fluctuating signal extraction. *Opt. Express* **24**, 3037–3045 (2016).
60. Zou, L., Zhang, S., Wang, B. & Tan, J. High-order super-resolution optical fluctuation imaging based on low-pass denoising. *Opt. Lett.* **43**, 707–710 (2018).
61. Zhao, W. et al. Enhanced detection of fluorescence fluctuations for high-throughput super-resolution imaging. *Nat. Photon.* **17**, 806–813 (2023).
62. Grußmayer, K. S. et al. Spectral cross-cumulants for multicolor super-resolved SOFI imaging. *Nat. Commun.* **11**, 3023 (2020).
63. Zhao, G., Zheng, C., Kuang, C. & Liu, X. Resolution-enhanced SOFI via structured illumination. *Opt. Lett.* **42**, 3956–3959 (2017).
64. Descloux, A. C. et al. Experimental combination of super-resolution optical fluctuation imaging with structured illumination microscopy for large fields-of-view. *ACS Photon.* **8**, 2440–2449 (2021).
65. Sroda, A. et al. SOFISM: super-resolution optical fluctuation image scanning microscopy. *Optica* **7**, 1308–1316 (2020).
66. Choi, Y. et al. Wide-field super-resolution optical fluctuation imaging through dynamic near-field speckle illumination. *Nano Lett.* **22**, 2194–2201 (2022).
67. Schwartz, O. et al. Superresolution microscopy with quantum emitters. *Nano Lett.* **13**, 5832–5836 (2013).
68. Israel, Y., Tenne, R., Oron, D. & Silberberg, Y. Quantum correlation enhanced super-resolution localization microscopy enabled by a fiber bundle camera. *Nat. Commun.* **8**, 14786 (2017).
69. Tenne, R. et al. Super-resolution enhancement by quantum image scanning microscopy. *Nat. Photon.* **13**, 116–122 (2019).
70. Lubin, R., Antolovic, I. M., Charbon, E., Bruschini, C. & Oron, D. Quantum correlation measurement with single photon avalanche diode arrays. *Opt. Express* **27**, 32863–32882 (2019).
71. Rossman, U. et al. Rapid quantum image scanning microscopy by joint sparse reconstruction. *Optica* **6**, 1290–1296 (2019).
72. Weisenburger, S. et al. Cryogenic colocalization microscopy for nanometer-distance measurements. *ChemPhysChem* **15**, 763–770 (2014).
73. Weisenburger, S. et al. Cryogenic optical localization provides 3D protein structure data with angstrom resolution. *Nat. Methods* **14**, 141–144 (2017).
74. Böning, D., Wieser, F.-F. & Sandoghdar, V. Polarization-encoded colocalization microscopy at cryogenic temperatures. *ACS Photon.* **8**, 194–201 (2021).
75. Perez, D. et al. Identification and demonstration of roGFP2 as an environmental sensor for cryogenic correlative light and electron microscopy. *J. Struct. Biol.* **214**, 107881 (2022).
76. Sartor, A. M., Dahlberg, P. D., Perez, D. & Moerner, W. E. Characterization of mApple as a red fluorescent protein for cryogenic single-molecule imaging with turn-off and turn-on active control mechanisms. *J. Phys. Chem. B* **127**, 2690–2700 (2023).
77. Moser, F. et al. Cryo-SOFI enabling low-dose super-resolution correlative light and electron cryo-microscopy. *Proc. Natl Acad. Sci. USA* **116**, 4804–4809 (2019).
78. Gustafsson, N. et al. Fast live-cell conventional fluorophore nanoscopy with ImageJ through superresolution radial fluctuations. *Nat. Commun.* **7**, 12471 (2016).
79. Vandenberg, W., Leutenegger, M., Duwé, S. & Dedecker, P. An extended quantitative model for super-resolution optical fluctuation imaging (SOFI). *Opt. Express* **27**, 25749–25766 (2019).

80. Han, Y. et al. Ultrafast, universal super-resolution radial fluctuations (SRRF) algorithm for live-cell super-resolution microscopy. *Opt. Express* **27**, 38337–38348 (2019).
81. Venkatachalapathy, M., Belapurkar, V., Jose, M., Gautier, A. & Nair, D. Live cell super resolution imaging by radial fluctuations using fluorogen binding tags. *Nanoscale* **11**, 3626–3632 (2019).
82. Wang, B. et al. Multicomposite superresolution microscopy: enhanced Airyscan resolution with radial fluctuation and sample expansions. *J. Biophoton.* **13**, e2419 (2020).
83. Ehrlich, R. et al. Super-resolution radial fluctuations (SRRF) nanoscopy in the near infrared. *Opt. Express* **30**, 1130–1142 (2022).
84. Gong, X. et al. Achieving increased resolution and reconstructed image quality with intensity and gradient variance reweighted radial fluctuations. *ACS Photon.* **9**, 1700–1708 (2022).
85. Solano, A., Lou, J., Scipioni, L., Gratton, E. & Hinde, E. Radial pair correlation of molecular brightness fluctuations maps protein diffusion as a function of oligomeric state within live-cell nuclear architecture. *Biophys. J.* **121**, 2152–2167 (2022).
86. Tsutsumi, M., Takahashi, T., Kobayashi, K. & Nemoto, T. Fluorescence radial fluctuation enables two-photon super-resolution microscopy. *Front. Cell. Neurosci.* **17**, 1243633 (2023).
87. Laine, R. F. et al. High-fidelity 3D live-cell nanoscopy through data-driven enhanced super-resolution radial fluctuation. *Nat. Methods* **20**, 1949–1956 (2023).
88. Chen, J. et al. Deep-learning accelerated super-resolution radial fluctuations (SRRF) enables real-time live cell imaging. *Opt. Lasers Eng.* **172**, 107840 (2024).
89. Li, Y., Liu, L., Roberts, S. K. & Wang, L. Super-resolution radial fluctuations microscopy for optimal resolution and fidelity. *Opt. Lett.* **49**, 2621–2624 (2024).
90. Shaib, A. H. et al. One-step nanoscale expansion microscopy reveals individual protein shapes. *Nat. Biotechnol.* https://doi.org/10.1038/s41587-024-02431-9 (2024).

Acknowledgements

N.R. and J.E. acknowledge financial support from the Bundesministerium für Bildung und Forschung (BMBF) of Germany via project NG-FLIM (project no. 13N15327). J.I.G. acknowledges financial support from the European Union's Horizon 2021 research and innovation programme under the Marie Skłodowska-Curie grant agreement no. 101062508 (project name SOADOPP). I.Gligonov acknowledges funding from the International Max Planck Research School for Physics of Biological and Complex Systems and by the European Union via the HORIZON–MSCA–2022–DN 'Improving BiomEdical diagnosis through LIGHT-based technologies and machine learning—BE-LIGHT' (grant agreement no. 101119924–BE-LIGHT). J.E. and J.I.G. acknowledge financial support from the DFG through Germany's Excellence Strategy EXC 2067/1390729940. S.B., O.N., N.R. and J.E. thank the European Research Council (ERC) for financial support via project 'smMIET' (grant agreement no. 884488) under the European Union's Horizon 2020 research and innovation programme.

Author contributions

J.E. wrote the manuscript. A.C. and J.E. generated all the figures. S.B., J.I.G., I. Gregor, O.N. and R.T. proofread the final version of the manuscript, and checked the correctness of all citations. N.R. performed the measurements for Fig. 3c. I. Gligonov checked all the theoretical equations in the manuscript.

Competing interests

The authors declare no competing interests.

Additional information

Correspondence and requests for materials should be addressed to Jörg Enderlein.

Peer review information *Nature Photonics* thanks Mike Heilemann and the other, anonymous, reviewer(s) for their contribution to the peer review of this work.